ELSEVIER

Journal of Nuclear Materials 290–293 (2001) 867–871

journal of nuclear materials

www.elsevier.nl/locate/jnucmat

Noble gas enrichment studies at JET

M. Groth [a,*], P. Andrew [b], W. Fundamenski, H.Y. Guo [c], D.L. Hillis [d], J.T. Hogan [d], L.D. Horton [e], G.F. Matthews, A.G. Meigs, P.M. Morgan, M.F. Stamp, M. von Hellermann [f]

Jet Joint Undertaking, Abingdon, OX14 3EA, UK
[a] *also University of Manchester (UMIST), Manchester M60 1QD, UK*
[b] *University of Wisconsin, Madison, WI, USA*
[c] *Redmond Plasma Physics Laboratory, University of Washington, WA, USA*
[d] *Oak Ridge National Laboratory, Oak Ridge, TN, USA*
[e] *Max-Planck-Institut für Plasmaphysik Garching, Germany*
[f] *FOM Institute for Plasma Physics, Rijnhuizen, Nieuwegein, Netherlands*

Abstract

Adequate helium exhaust has been achieved in reactor-relevant ELMy H-mode plasmas in JET performed in the MKII AP and MKII GB divertor geometry. The divertor-characteristic quantities of noble gas compression and enrichment have been experimentally inferred from Charge Exchange Recombination Spectroscopy measurements in the core plasma, and from spectroscopic analysis of a Penning gauge discharge in the exhaust gas. The retention of helium was found to be satisfactory for a next-step device, with enrichment factors exceeding 0.1. The helium enrichment decreases with increasing core plasma density, while the neon enrichment has the opposite behaviour. Analytic and numerical analyses of these plasmas using the divertor impurity code package DIVIMP/NIMBUS support the explanation that the enrichment of noble gases depends significantly on the penetration depth of the impurity neutrals with respect to the fuel atoms. Changes of the divertor plasma configuration and divertor geometry have no effect on the enrichment. © 2001 Published by Elsevier Science B.V.

Keywords: Particle compression; Impurity enrichment; Divertor leakage; Ionization mean free path

1. Introduction

In fusion devices of significant alpha-particle production, adequate removal of the deuterium-tritium (D–T) reaction ash, helium (He), is required to maintain sufficient core plasma purity. For the ultimate removal of helium from the system, a sufficiently large neutral helium pressure and adequate pumping facilities in the exhaust channel of the reactor are needed.

Advanced operational scenarios in tokamaks comprise the introduction (seeding) of impurities, to reduce the power flowing onto the target plates in a diverted magnetic configuration to technically feasible levels [1]. In particular, the noble gases neon (Ne), argon (Ar) and krypton (Kr) are suitable candidates for such seeding, as their wall recycling properties enable better particle control than more volatile gases, such as methane.

In diverted magnetic configurations, the retention efficiency of impurity particles of a divertor is characterised by the impurity compression and impurity enrichment. The compression factor is defined as the ratio of the neutral density in the exhaust gas to the ion density of the same species in the core plasma, i.e.,

$$C = \frac{n_0^{\mathrm{subdiv}}}{n_+^{\mathrm{core}}}, \quad (1)$$

whereby the core ion density can refer to various normalised radii, ρ; here it carries the value at $\rho \sim 0.9$.

* Corresponding author. Culham Research Centre, Abingdon, OX14 3EA, UK. Tel.: +44-1235 464 779; fax: +44-1235 464 535.

E-mail address: mgroth@jet.uk (M. Groth).

0022-3115/01/$ - see front matter © 2001 Published by Elsevier Science B.V.
PII: S0022-3115(00)00652-8

Strictly, to characterise the divertor, the compression factors should refer to the divertor densities; however, since there are no direct divertor density measurements available, the neutral densities in the exhaust are used instead. The enrichment factor is defined as the ratio of the impurity compression to the compression of the D–T fuel, i.e.,

$$\eta_{\mathrm{imp}} = \frac{C_{\mathrm{imp}}}{C_{\mathrm{D-T}}}. \quad (2)$$

To satisfy the requirement of high core plasma purity, large impurity compression and enrichment factors above unity are desired, while keeping the D–T throughput simultaneously as small as possible. Following recent design studies on ITER [2], a dilution of helium in the exhaust can still be tolerated, permitting a helium enrichment larger than 0.1. Investigations in the enrichment of He at various experimental tokamaks have indicated that this requirement can be met in standard low (L-mode) and high confinement (H-mode) discharges [3–6].

2. Experimental arrangement

To experimentally derive the retention properties of divertors as defined above, at JET the charge exchange recombination spectroscopy (CXRS) system [7] is used to determine the impurity densities of helium and neon at 10 radial positions across the plasma cross-section. The impurity density profiles of interest are inferred from CXRS measurements of the line intensities in the visible wavelength range for HeII at 468.6 nm and NeX at 524.9 nm.

To obtain the neutral densities in the subdivertor, a spectroscopic technique utilising Penning gauges [8,9] has been adopted which is based on the excitation of the neutral gas in a Penning gauge. Here, a photomultiplier-interference filter arrangement was used to measure the line intensity of HeI at 587.5 nm and NeI 640.4 nm. Furthermore, the D_α (656.1 nm) transition was used for deuterium measurements. As shown in Fig. 1, the Penning gauges, of type ALCATEL CF2P, are mounted at the far end of a vacuum tube, approximately 2.5 m below the JET subdivertor.

Under standard operation the JET divertor cryopump is cooled to 4.7 K using liquid helium, which permits pumping of the deuterium fuel and neon. Unless an argon frost layer is applied to the cryopump panels, helium cannot be pumped. Since this operation directly affects the neutral densities in the subdivertor, a few discharges in the MKII GB campaign were performed utilising an argon frost technique [10]. The helium compression and enrichment quoted here are based on

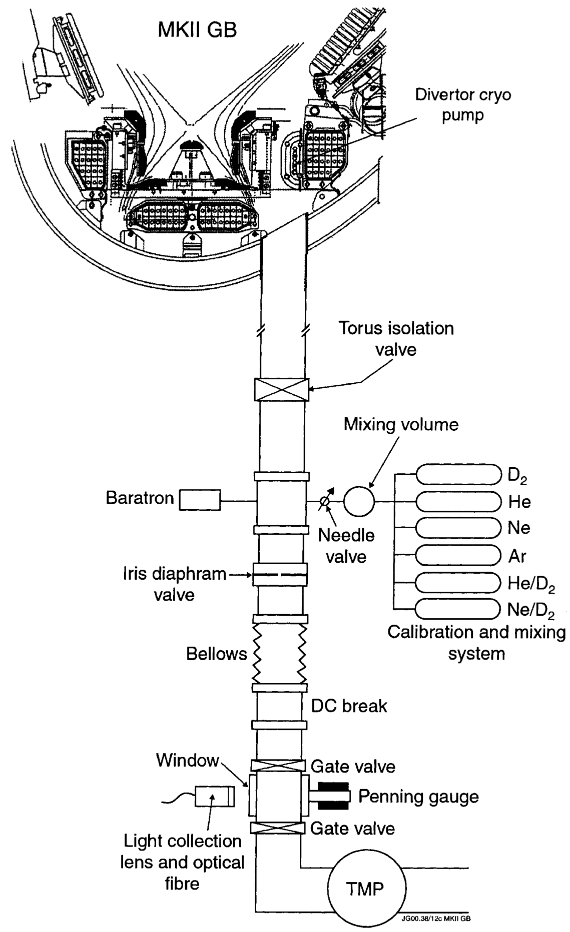

Fig. 1. The JET Penning gauge diagnostic attached to the subdivertor chamber. The baratron and the in-situ gas calibration system were installed for calibration purpose.

discharges without active helium pumping, unless otherwise stated.

Experimentally, helium and neon were injected as neutral gas via short puffs or bleeds from a gas module at the main chamber mid-plane. The range of plasmas investigated encompasses L-mode and ELMy H-mode discharges with attached and partially detached divertor plasmas.

3. Experimental results and their interpretation

From zero-dimensional considerations, the most influential factors on impurity compression and enrichment are the recycling properties, determining how the neutrals emerge from the target plates, and the divertor background plasma conditions, i.e., the divertor density, $n_{\mathrm{e,div}}$, and temperature, $T_{\mathrm{e,div}}$ [11,12]. Experimentally, the

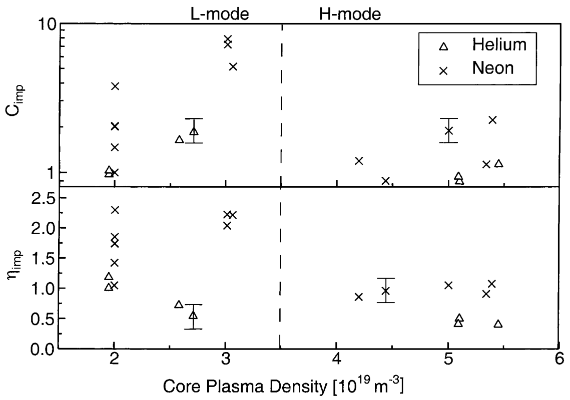

Fig. 2. Helium and neon compression and enrichment factors obtained in the MKII GB divertor geometry.

latter parameters have been changed by altering the upstream, core plasma density, $\langle n_e \rangle$.

As shown in Fig. 2 for the MKII GB divertor geometry, the impurity compression factors typically increase with core plasma density, extending from unity to 2 for helium, and up to 10 for neon. However, the helium enrichment decreases with density and is found to be larger than 0.1 in reactor-relevant ELMy H-mode discharges under active helium pumping conditions. The neon enrichment, in contrast, increases with density, exceeds unity and can be as large as 2.5.

The opposite behaviour of the enrichment for the two impurity species suggests that the leakage of impurities out of a divertor is either dominated by atom or ion transport, signified by on the ionisation mean free path of the impurities and D–T fuel. For simplicity it is here assumed that neutrals are ionised by electron impact only, so that the ionisation mean free path, λ_{n-e}, can be written as

$$\lambda_{n-e} = \frac{v_0}{n_{e,div} \langle \sigma v_e \rangle (T_e)}, \qquad (3)$$

where v_0 is the velocity of the neutrals, and $\langle \sigma v_e \rangle$ is the ionisation rate coefficient. The long ionisation mean free path of helium, of typically a few centimetres, allows the helium atoms to escape from the divertor plasma as neutrals, whereas neon is ionised already within a few millimetres. Even though $n_{e,div}$ is higher at larger $\langle n_e \rangle$, the dependence of λ_{n-e} on $T_{e,div}$ is much stronger, causing λ_{n-e} to be longer at larger $\langle n_e \rangle$.

Consequently, the divertor leakage for helium can be described by a divertor neutral model, introduced in the following section. The leakage of neon has been explained in an one-dimensional ion transport model, introduced by Neuhauser [11], which is based on the balance of friction and temperature gradients forces arising due to collisions of the impurity ion with electrons and ions of the background plasma. Following the Neuhauser model, the leakage of neon ions is more suppressed at larger $n_{e,div}$, leading to larger neon enrichment factors, as observed.

The dependence of the helium compression and enrichment on divertor geometry has been investigated in the MKII AP and the MKII GB divertor geometry [13]. The MKII GB divertor geometry is characterised by a more closed geometrical structure preventing neutrals to escape from the divertor chamber into the tokamak main chamber. Increased neutral densities in the divertor chamber under otherwise similar core plasma condition have been obtained in the MKII GB compared to the MKII AP divertor [14]. Consequently, the helium compression was improved in the MKII GB geometry, thus enhancing the pumping capability. However, as a similar background plasma was obtained in both divertor geometries for corresponding core plasma conditions, the enrichment of helium was unaffected, in accordance with the divertor neutral model.

The effect of the divertor plasma configuration on the helium compression and enrichment has been extensively studied in L-mode in the MKII AP divertor geometry [15]. The three magnetic configurations achieved differ in the position where the plasma strike zones are attached to the target plates, with respect to the pumping slots location: horizontal, corner and vertical configuration. In particular in the corner configuration, neutral particles emerging from strikes zones have maximum probability to reach the subdivertor via the corner slots. This fact is reflected by the largest compression of helium obtained in the corner configuration, while the horizontal and vertical configuration exhibit similar compression factors. However, variations of the strike zone position did not affect the helium enrichment.

4. Divertor neutral model and DIVIMP modelling

A zero-dimensional model [16] that describes the escape of neutral particles from a divertor plasma can be used to explain the observation on the helium enrichment. This model is schematically drafted in Fig. 3 and is based on the flow of particles into and out of the divertor chamber. To prevent particle accumulation in the divertor chamber, the flow, Γ_+, of plasma ions of any species streaming into the divertor volume must be balanced by an outflow, Γ_0, of neutral particles back into the main chamber or into the subdivertor volume. Escape of ions out of the divertor volume is entirely neglected in this model. To quantify the escape of neutrals into the main chamber and subdivertor, the probabilities P_{back} and P_{pump} are attributed to each escape route, respectively. In steady-state, the flow balance can be written as

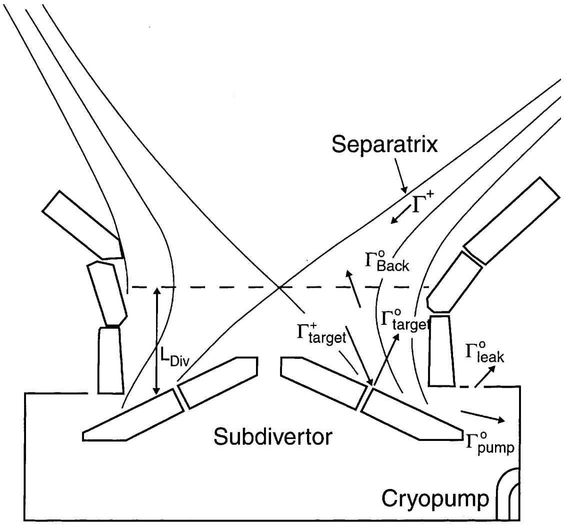

Fig. 3. Schematic sketch of the divertor neutral model.

$$\Gamma_+ = \lfloor (1 - P_{\rm pump}) P_{\rm back} + P_{\rm pump} \rfloor \Gamma_0. \qquad (4)$$

As the flow into the subdivertor is small, $P_{\rm back} \ll P_{\rm pump}$, the particle compression factor can be simplified to

$$C = 1/P_{\rm back} \cdot v_+/v_0 \cdot A_{\rm eff,up}/A_{\rm eff,div}, \qquad (5)$$

where v_+ and v_0 are the ion and neutral flow velocities and $A_{\rm eff}, *$ is the effective area in the upstream and divertor scrape-off layer, respectively. Assuming that the flow velocities of deuterium and helium into the divertor are approximately the same, i.e., neglecting flow reversal, the helium enrichment factor can be derived as

$$\eta_{\rm He} \approx P_{\rm back,D}/P_{\rm back,He} \cdot v_{0,\rm He}/v_{0,D}. \qquad (6)$$

Under typical divertor conditions, noble gases can be assumed to be thermally released from the target, yielding a kinetic energy of 0.04 eV corresponding to the wall temperature [17]. As deuterium molecules are subject to Franck–Condon dissociation, the resulting deuterium atoms have much larger kinetic energies, of approximately 2–3 eV. Hence, the ratio of the velocities of helium and deuterium atoms does not vary significantly with changes in the background plasma, so that the helium enrichment factor depends merely on the probability with which the atoms of both species can return to the main chamber. As these probabilities are related to the ionisation mean free paths, i.e., $P_{\rm back} \propto \exp(-L_{\rm Div}/\lambda_{\rm n-e})$, the helium enrichment factor yields the proportionality,

$$\eta_{\rm He} \propto \exp\left(\frac{L_{\rm Div}}{\lambda_{\rm e-n,D}\lambda_{\rm e-n,He}}(\lambda_{\rm e-n,D} - \lambda_{\rm e-n,He})\right), \qquad (7)$$

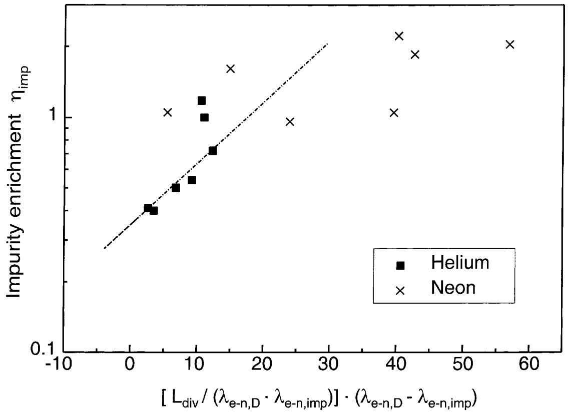

Fig. 4. Experimentally obtained impurity enrichment factors plotted as a function of the scaling suggested by the divertor neutral model.

where $L_{\rm Div}$ denotes a characteristic dimension of the divertor. According to Eq. (7), the greater the difference between the ionisation front of deuterium and helium the larger the helium enrichment. Using the target density and temperature measured by the JET Langmuir probe array, the ionisation mean free path has been calculated and substituted into Eq. (7). Under JET divertor conditions approaching plasma detachment, i.e. $n_{\rm e,div} > 5 \times 10^{19}$ m^{-3} and $T_{\rm e,div} < 10$ eV, the ionisation length of deuterium and helium become comparable, hence the divertor plasma becomes more and more transparent to helium atoms, and the helium enrichment decreases as shown in Fig. 4.

Detailed two-dimensional DIVIMP/NIMBUS [12], [18] simulations on helium and neon divertor and edge transport support these interpretations. The Langmuir probe measurements at the target plates were used as input parameters for the background plasma. Furthermore, a constant perpendicular diffusion coefficient $D_\perp = 0.1$ m^2 s^{-1} and a trivial pinch velocity, i.e., $v_{\rm pinch} = 0$, for the impurity ions were assumed. The recycling of both noble gases was simulated by re-injecting these particles in a cosine velocity distribution of kinetic energy 0.04 eV. As DIVIMP does not follow impurity particles into the subdivertor, an analytic neutral transport model was coupled to the solution of DIVIMP/NIMBUS to derive the partial impurity pressures in the pumping chamber. Good agreement between the experimental and numerical results has been achieved, in particular the opposite dependence of the helium and neon enrichment on $\langle n_{\rm e} \rangle$ has been reproduced (Fig. 5). In addition, a comparison of the numerical results confirmed that the helium enrichment factors are virtually the same for the MKII AP and MKII GB divertor geometry and unaffected by the divertor plasma configuration.

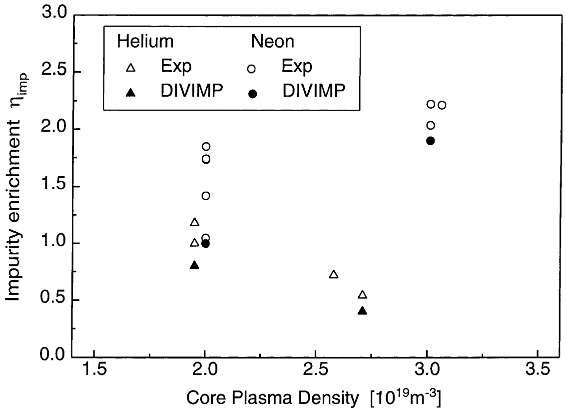

Fig. 5. Comparison between the measured and numerically calculated impurity enrichment factors in L-mode plasmas in the MKII AP and MKII GB divertor geometry.

5. Conclusions

The compression and enrichment of the noble gases helium and neon have been studied in the JET MKII AP and MKII GB divertor geometry under a variety of core and divertor plasma conditions. Adequate impurity retention has been achieved for both species, in particular the helium enrichment exceeds the value of 0.1 required in a next-step fusion device. While the compression ratio of both noble gases increase with core plasma density in L-mode and ELMy H-mode plasmas, lower helium enrichment and higher neon enrichment factors have been measured at larger core plasma densities. This phenomenon can be explained by the difference in the ionisation mean free paths of helium and neon. It can be argued that helium escapes predominately atomic while neon leakage from the divertor is an ion transport process. Consequently, for a next-step fusion device an adequately opaque divertor plasma is essential. Detailed DIVIMP/NIMBUS simulations have confirmed this interpretation.

A comparison of the helium enrichment on the location of the plasma strike zones with respect to the divertor pumping slots and the divertor geometry has indicated that these parameters do not influence the divertor leakage of helium. In contrast, the largest helium compression factors of about 2 have been achieved in the corner plasma configuration in the MKII AP divertor geometry and in the MKII GB divertor geometry. Hence, a divertor with a closed geometry and the strike zone adjacent to the pumping slots enhance the helium throughput at the pump.

References

[1] G. Janeschitz, ITER–JCT and Home Teams, Plasma Phys. Control. Fus. 37 (1995) A19.
[2] A. Kukushin et al., in: Proceedings of the 26th EPS Conference on Controlled Fusion in Plasma Physics, Maastricht, Netherlands, vol. 23J, 1999, p. 1545.
[3] J.A. Goetz et al., J. Nucl. Mater. 266–269 (1999) 354.
[4] H.-S. Bosch, in: J.T. Hogan, D.L. Hillis, (Eds.), Conference report: Helium transport and exhaust in tokamaks, Nucl. Fus., 40, 879.
[5] M.R. Wade, Nucl. Fus. 38 (1998) 1839.
[6] A. Sakasai et al., J. Nucl. Mater. 266–269 (1999) 1839.
[7] M. von Hellermann et al., Active Beam Spectroscopy in JET, Elsevier, Amsterdam, 1993, p. 142.
[8] A. Hardtke, Ph.D. thesis, University of Essen, 1989.
[9] K.H. Finken et al., Rev. Sci. Instrum. 63 (1992) 1.
[10] D. Stork et al., in: Proceedings of the 26th EPS Conference on Controlled Fusion in Plasma Physics, Maastricht, Netherlands, vol. 23J, 1999, p. 205.
[11] J. Neuhauser et al., Nucl. Fus. 24 (1984) 39.
[12] P.C. Stangeby et al., Nucl. Fus. 35 (1995) 1391.
[13] G.C. Vlases et al., J. Nucl. Mater. 266–269 (1999) 160.
[14] R.D. Monk et al., Nucl. Fus. 11Y (1999) 1751.
[15] M. Groth et al., in: Proceedings of the 25th EPS Conference on Controlled Fusion in Plasma Physics, Prague, vol. 22C, 1998, p. 39.
[16] W. Ullrich, Ph.D. thesis, University of Augsburg, 1999.
[17] W. Eckstein et al., in: R. Janev (Ed.), Nucl. Fus. (special issue) 1991.
[18] E. Cupini et al., NET XII-324/9 Report, 1984.